Thermochimica Acta, 153 (1989) 47–61
Elsevier Science Publishers B.V., Amsterdam – Printed in The Netherlands

THERMOCHEMICAL CHARACTERIZATION OF ULTRAFINE Sr-HEXAFERRITE *

S.D. KULKARNI, C.E. DESHPANDE, J.J. SHROTRI, V.G. GUNJIKAR
and S.K. DATE **

Physical Chemistry Division, National Chemical Laboratory, Pune 411 008 (India)

(Received 13 February 1989)

ABSTRACT

Thermal (DTA/DTG/TG) studies have been carried out in order to understand the ferritization reaction leading to the formation of hexagonal strontium ferrite. Two different routes, namely, (a) the conventional ceramic method (solid state reaction) and (b) the chemical coprecipitation method, have been used to prepare the starting materials. Simultaneous DTA/DTG/TG plots clearly exhibit the onset of the exothermic ferritization reaction at $T \simeq 730$ °C, with an activation energy of 43.872 kcal mol^{-1} for the precursors derived from the coprecipitation route. On the other hand, the temperature required for the reaction with the ceramic route precursors was greater than 900 °C without any accompanying energy change.

INTRODUCTION

Hard ferrites are one of the major components in the field of high-tech ceramics. In this exciting area, the key to success in achieving high performance parameters is to prepare highly uniform and ultrafine particles and their subsequent processing. Various preparation methods such as the powder metallurgical method [1], the chemical coprecipitation method [2–4], the glass crystallization method [5,6], the organic resin method [7], the liquid mix technique [8,9], the sol–gel technique [10,11], the hydrothermal method [12], etc. have been explored to control the microstructure of the green body. In an earlier communication [13], the synthesis of high performance Sr-hexaferrite prepared by the chemical coprecipitation method was reported. On low temperature processing of this precipitate under optimum conditions, excellent magnetic parameters for the dense compact were achieved, i.e. (BH) ≃ 1.6 MGOe and Br = 2750 G.

---

* NCL Communication No. 4630.

** Author to whom correspondence should be addressed.

0040-6031/89/$03.50

However, it has been noticed that the mechanism governing the ferritization reaction during these processing experiments is poorly understood and varied and often contradictory observations [9,14–17] regarding the nature of the reaction have been reported. For example, a few researchers have failed to observe any energy change during the ferritization reaction, while Roos [14] and Higuchi et al. [15] observed an exothermic peak at around 750 ° C. Thermal analysis is rarely used for investigating the formation of ferrite in comparison with other methods of analysis, and because the thermochemical data so far reported is mainly on Ba-hexaferrite, an analysis of the reaction in the case of Sr-hexaferrite is attempted here. In continuation with the earlier research work performed in our laboratory [13,18], we report in the following a detailed analysis of the thermal data obtained from a systematic DTA/DTG/TG study of the two preparation methods for Sr-hexaferrite, namely, ceramic and coprecipitation.

EXPERIMENTAL

Preparation

Sr-hexaferrite was prepared by two different techniques, namely, (a) ceramic and (b) chemical coprecipitation, using the following raw materials: α-Fe_2O_3 and $SrCO_3$ (commercial grade); $FeCl_3 \cdot 6H_2O$ (LR grade, SD Fine Chemicals, India); $SrCl_2 \cdot 6H_2O$ (LR grade, Ranbaxy, India); and NaOH (LR grade, SD Fine Chemicals, India).

Figure 1 gives a flow chart illustrating the preparation processes. Hexagonal ferrite was prepared by keeping the molar ratio of Fe/Sr = 11 in both the techniques, the detailed preparation procedure being described elsewhere [18].

Instrumental

As described in Fig. 1, the samples were characterized during different stages of their synthesis using DTA, XRD, IR and SEM techniques.

Thermal analysis (DTA / DTG / TG)

A Netzsch STA 409 differential thermal analyser was used to locate the reaction temperature, i.e. the onset of the ferritization reaction for the two different preparation methods and to study their thermochemical behaviour. A calibrated Pt/Pt–10% Rh thermocouple was used for sensing the temperature accurately. The samples were heated in dynamic air with a heating rate of 10 ° C min^{-1} and a chart speed of 120 mm h^{-1} during the full scan (20–1400 ° C). Three types of thermal scans were taken:

1. A normal DTA/DTG/TG scan for i) the physical mixture of α-Fe_2O_3 and $SrCO_3$ and ii) the coprecipitate of Fe and Sr hydroxides;

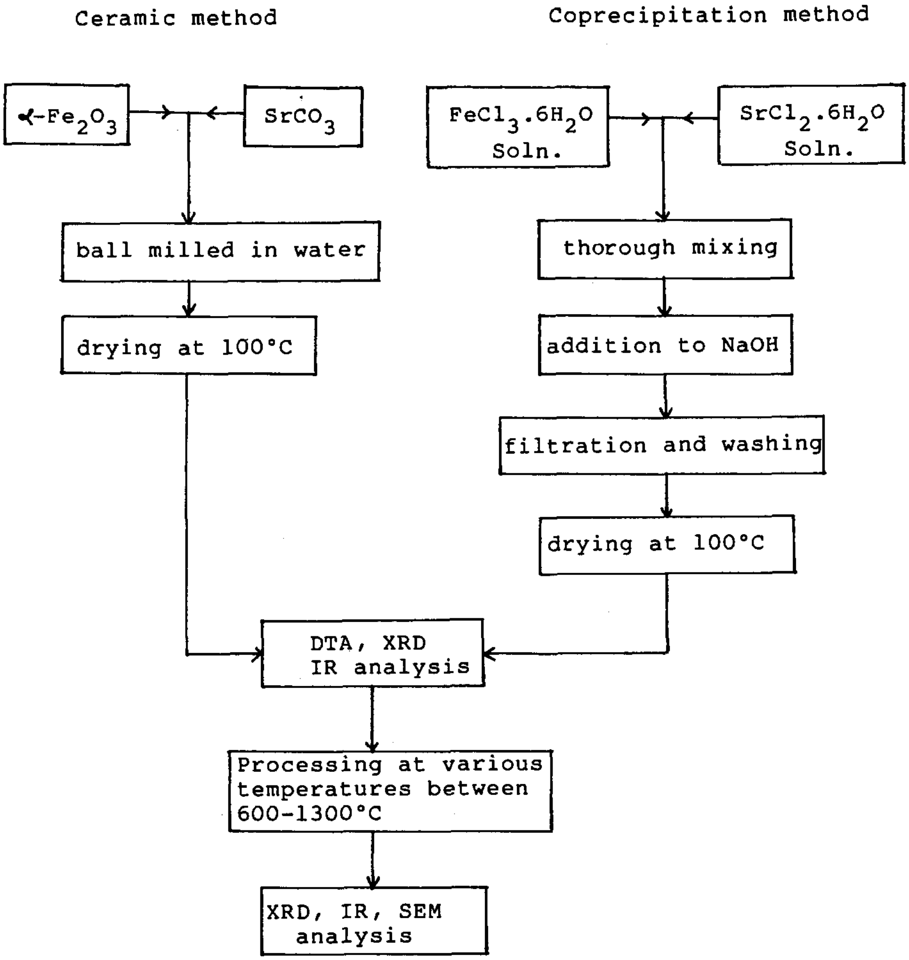

Fig. 1. Flow chart showing preparation procedures of $SrFe_{12}O_{19}$ from ceramic and coprecipitation methods.

2. DTA/DTG/TG scans for the coprecipitate with various heating rates between 2°C min^{-1} and 50°C min^{-1}; and
3. An isothermal DTA scan for the mixture of α-Fe_2O_3 and $SrCO_3$ at 900°C for 6 h.

XRD

A Philips PW 1730 X-ray diffractometer using Cu $K\alpha$ radiation ($\lambda = 1.542$ Å) was used for recording the powder spectra of the samples prepared by the two techniques.

IR

IR spectra of samples were recorded in Nujol on a Pye–Unicam IR Spectrometer (SP3-300).

SEM

The particle size and its distribution, and the morphology of the samples were observed on a Cambridge Stereoscan 150 scanning electron microscope.

RESULTS AND DISCUSSION

Thermal analysis

Figure 2a gives the thermograms of the mixture of α-Fe_2O_3 and $SrCO_3$ between 20 and 1400 °C. 40.2 mg samples of the mixture of α-Fe_2O_3 and $SrCO_3$ were used for the thermal measurements. The TG curve shows a continuous slow rise up to 640 °C without any change in the DTG curve. This change, therefore, was attributed to the buoyancy effect and can be considered to be negligible. The main decomposition starts from 710 °C onwards up to 1070 °C which was evident from the two small peaks in the DTG curve at 810 and 970 °C, with a total weight loss of 3.11%. The DTA curve shows a broad endotherm up to 1200 °C with a small hump at $\simeq$ 960 °C. However, no exothermic energy change associated with the ferritization reaction was observed in the temperature range between 1000 and 1380 °C. The peaks at 810 and 970 °C can be attributed to the decomposition stages of $SrCO_3$ [19].

For preparation using the coprecipitation route, an exact sample (100 mg) was used for thermal studies. Figure 2b describes the thermal behaviour of the coprecipitate between 20 and 1200 °C. A sharp weight loss of $\simeq$ 16.4% was observed up to 568 °C due to the loss of water molecules. The DTA plot showed an endothermic peak at 126 °C corresponding to this loss. With the increase in temperature, an exothermic peak appeared at 730 °C indicating the onset of some chemical change in the coprecipitate. This can be attributed to the ferritization reaction as was demonstrated by the appearance of Sr-hexaferrite peaks in the XRD pattern of the coprecipitated sample heated at 750 °C over 5 h, as shown later in Fig. 6. Table 1 summarizes the thermal decomposition data for Sr-hexaferrite samples prepared by the two routes.

In order to calculate the activation energy of the ferritization reaction, DTA scans of 100 mg of the coprecipitated sample were taken at various rates, namely, 2, 5, 10, 20 and 50 °C min^{-1}. As the heating rate was increased, the exothermic peak appeared on the higher temperature side, successively. Figure 3 shows the plot of the logarithm of the heating rate against the inverse of the peak temperature. To calculate the activation energy, the following equation was used [20]

$$\log_{10} h = -\frac{E}{4.57} \times \frac{1}{T_{\mathrm{m}}} + \text{constant}$$

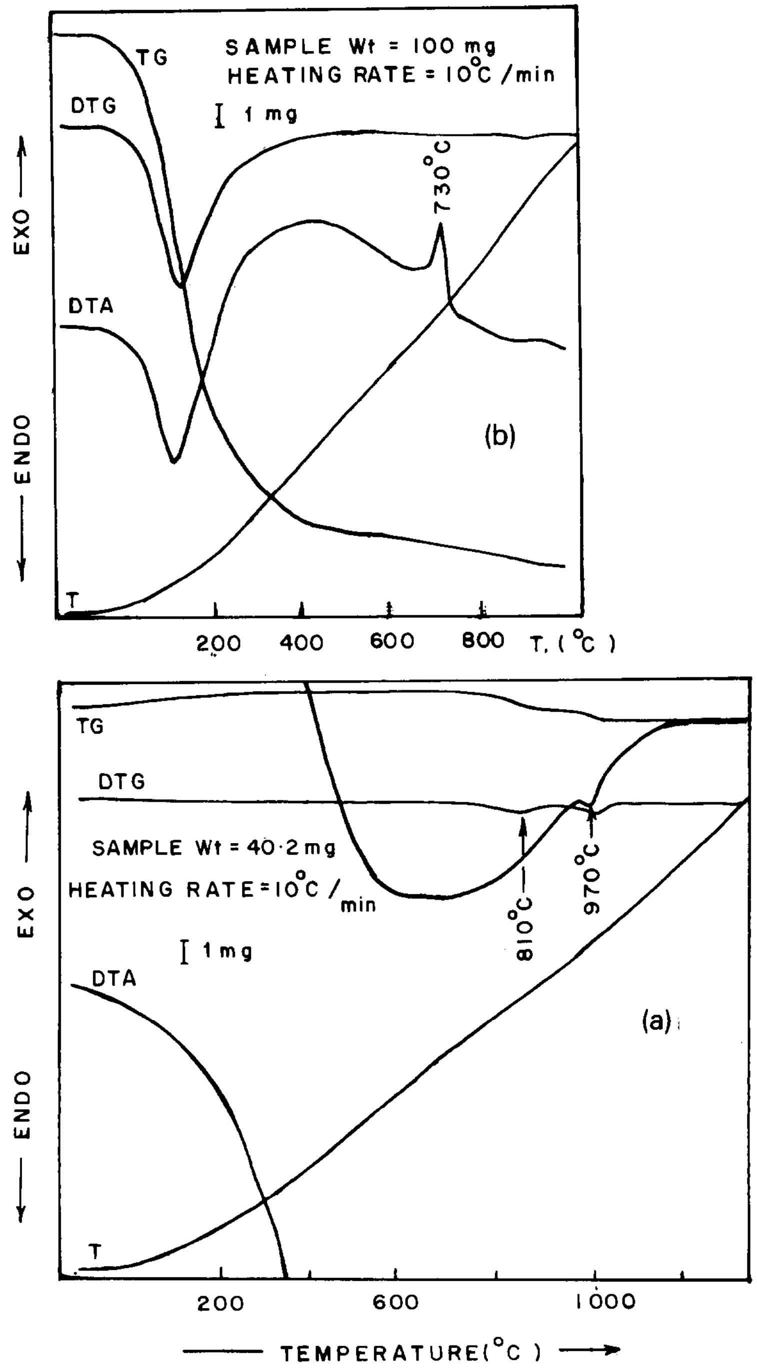

Fig. 2. Simultaneous DTA/DTG/TG curves of: a, the mixture of α-Fe_2O_3 and $SrCO_3$; b, the dried coprecipitate of Fe and Sr hydroxides.

TABLE 1

Thermal decomposition data for ceramic and coprecipitation methods

Method	DTA			DTG		TG % wt. loss	Associated change
	Peak temp. (° C)	Temp. range (° C)	Peak characteristics	Peak temp. (° C)	Temp. range (° C)		
Ceramic				810	710–910	3.11	Decomposition of $SrCO_3$
	960	910–990	Endothermic	970	910–990		Decomposition of $SrCO_3$
Coprecipitation	126	RT–450	Endothermic	126	RT–568	16.4	Loss of H_2O
	730	660–763	Exothermic	–	–	–	Ferritization reaction

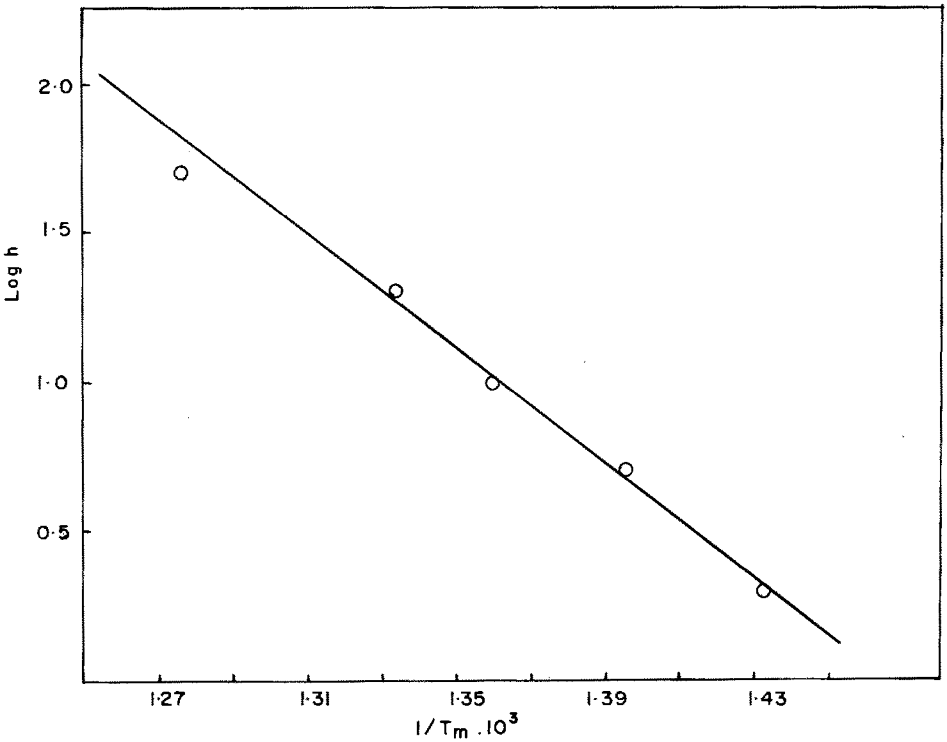

Fig. 3. Plot of $\log_{10} h$ versus $1/T_m$ (the values of T_m are read on DTA curves recorded at different heating rates, h, for the coprecipitated sample.)

where E is the activation energy, h is the heating rate and T_m is the peak temperature.

From the slope of the straight line, the activation energy was calculated to be 43.872 kcal mol^{-1}.

In the case of the ceramic preparation route, the DTA plot did not show any energy change up to 1380 °C. But the onset of the ferritization was observed at $T \geqslant 900$ °C, which will be substantiated later from the XRD data. The rate of reaction may be slow due to the larger and less active particles so that the corresponding energy change can be detected only if the reaction is carried out at the appropriate temperature for a longer time. To study this possibility, an isothermal scan was recorded on 48.8 mg of the physical mixture of α-Fe_2O_3 and $SrCO_3$ at 900 °C for 6 h, but the DTA plot did not show any exothermic energy change.

XRD and IR

To further investigate the nature of the ferritization reaction, a systematic study of the reaction has been carried out using XRD and IR techniques. Both the coprecipitate and the physical mixture of α-Fe_2O_3 and $SrCO_3$ were heated at various temperatures ranging from 600 to 1300 ° C, with steps of 100 ° successively, allowed to cool to room temperature and then analysed by the above two techniques.

Ceramic route

Figure 4 depicts the change in the X-ray diffraction patterns of the original reactants with the increase in temperature. Representative X-ray diffractograms are shown in the figure. It clearly exhibits Sr-hexaferrite peaks at around 900 ° C, along with the peaks of unreacted components: α-Fe_2O_3 being identified by the corresponding diffraction lines while Sr carbonate and/or oxide was not evident owing to their low concentration. A small amount of $SrFe_2O_4$ phase was also observed at 900 ° C which decreased with the increase in temperature, and, finally, single phase Sr-hexaferrite was formed at 1300 ° C. The formation of spinel ferrite intermediate phase during the reaction has been already reported by many authors [21].

Figure 5 gives the IR spectra of the sample formed from α-Fe_2O_3 and $SrCO_3$ when heated at various temperatures between 600 and 1300 ° C, along with that of the original physical mixture. In the 800–300 cm^{-1} region, the samples heated at $T \leqslant 800$ ° C showed α-Fe_2O_3 with its characteristic bands at $\simeq 545$, 470 and 330 cm^{-1}, while that of $SrCO_3$ is at 860 cm^{-1}. The pattern successively changed above 900 ° C, indicating chemical reaction between Fe_2O_3 and $SrO/SrCO_3$. The band at 860 cm^{-1} disappeared and the other peaks in the region of 600–300 cm^{-1} became broad and split. The completion of the reaction at 1300 ° C as indicated by XRD, was also confirmed by IR, showing double absorption peaks at 600 and 450 cm^{-1}. These were attributed to two kinds of Fe^{3+} sites: FeO in tetrahedral and FeO_6 in octahedral coordinations [15].

Coprecipitation route

The changes occurring in the XRD pattern during the heating of the coprecipitate at various temperatures from 600 up to 1300 ° C are shown in Fig. 6. It is clear from the accurate analysis of the intensities, that a temperature of $T \simeq 700$ ° C is required to start the ferritization, and 1200 ° C is necessary for complete conversion of oxides into the hexaferrite phase. There are also clear indications of the formation of $SrFe_2O_4$ at about 900 ° C; its concentration continued to decrease at higher temperatures and, at 1200 ° C, single phase Sr-hexaferrite was observed.

Figure 7 describes the changes in the IR spectra of the same samples. The inset of the figure shows that the fresh coprecipitate had bands at 3400 and 1610 cm^{-1} due to the stretching and bending vibration modes of water and structural hydroxyl groups [22]. These bands disappeared for the sample heated at 600 ° C, due to loss of water molecules. In the region between 800 and 300 cm^{-1}, strong absorption bands due to the iron–oxygen lattice vibrations were observed at around 570 and 435 cm^{-1} indicating the

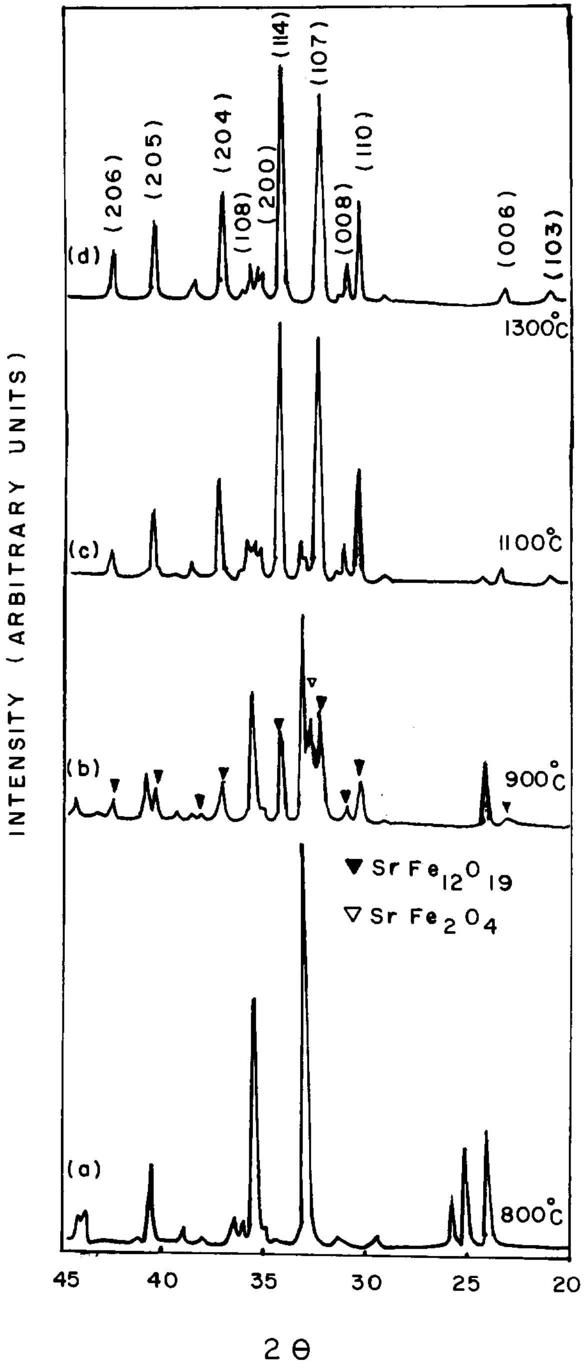

Fig. 4. X-ray diffraction patterns of the mixture of α-Fe_2O_3 and $SrCO_3$ heated at: a, 800 °C; b, 900 °C; c, 1100 °C; d, 1300 °C.

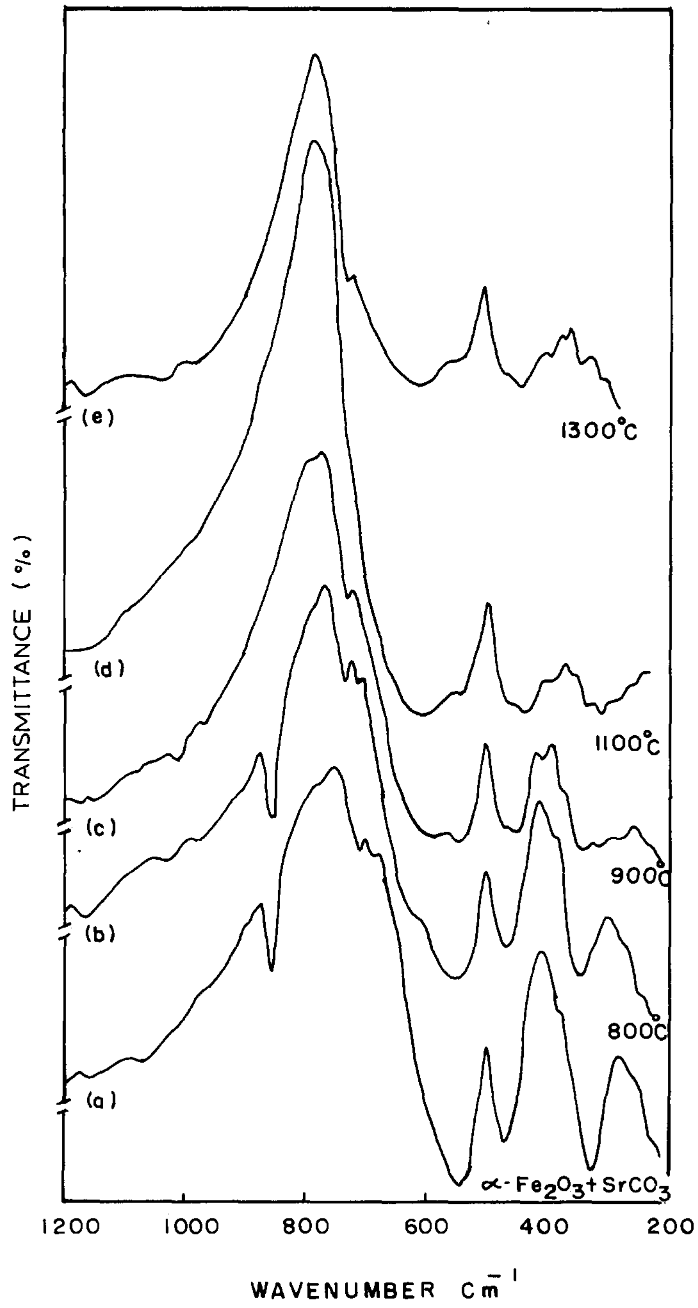

Fig. 5. IR spectra of: a, the mixture of α-Fe_2O_3 and $SrCO_3$; and the same calcined at: b, 800 ° C, c, 900 ° C; d, 1100 ° C; e, 1300 ° C.

presence of a hexagonal closed-packed arrangement of the oxygen sublattice, similar to that present in α-Fe_2O_3 and α-FeO · OH [23]. IR spectra for the samples heated at $T \geqslant 800\,°C$ exhibited broad and split bands. Ultimately

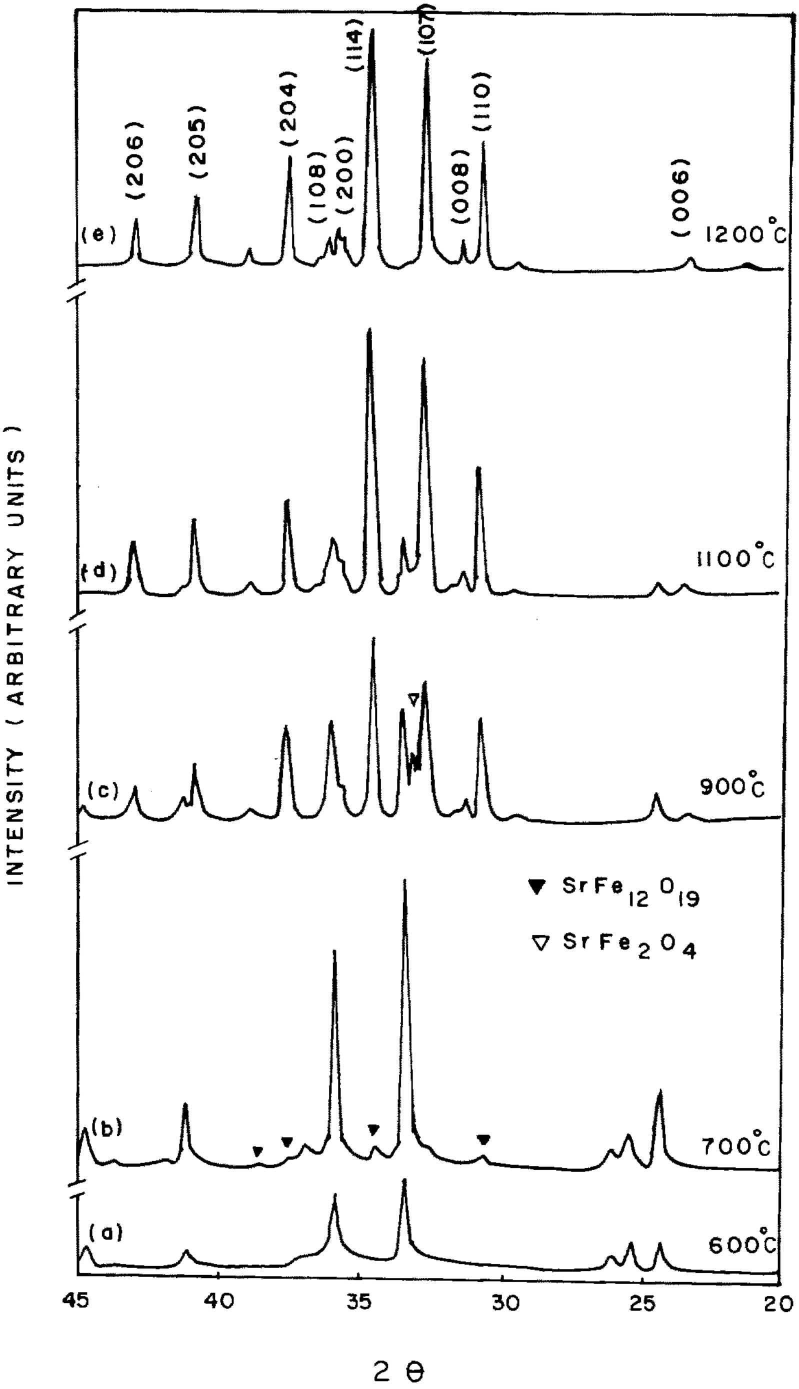

Fig. 6. X-ray diffraction patterns of the dried coprecipitate of hydroxides of Fe and Sr heated at: a, 600 ° C; b, 700 ° C; c, 900 ° C; d, 1100 ° C; e, 1200 ° C.

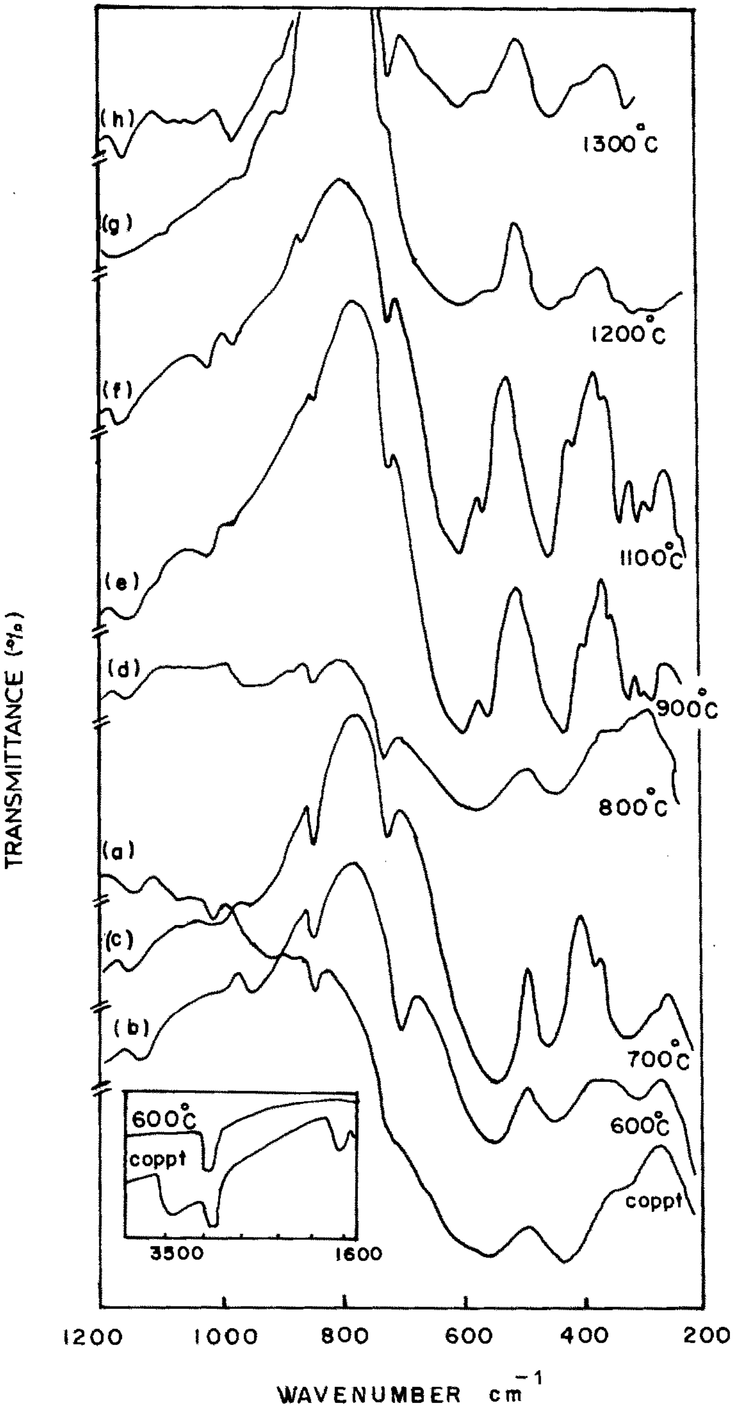

Fig. 7. IR spectra of: a, the dried coprecipitate of Fe and Sr hydroxides; and the same calcined at: b, 600 ° C; c, 700 ° C; d, 800 ° C; e, 900 ° C; f, 1100 ° C; g, 1200 ° C; h, 1300 ° C. Inset shows changes occurring in the bands of the coprecipitate when heated at 600 ° C, in the region 4000–1500 cm^{-1}.

two bands at 590 and 450 cm^{-1} were observed for the sample heated at 1200 °C at which temperature SR-hexaferrite has been fully formed. The spectrum matched well with that obtained using the ceramic method.

SEM

Figure 8 shows scanning electron micrographs of the sample heated at 750 °C for the coprecipitation method. It clearly shows particles of $\simeq 0.2$ μm, which are smaller than those produced by the ceramic method which has a particle size of $\geqslant 2$ μm [13].

It is clear from these experiments that, after decomposition of the original precursors, both the ceramic and coprecipitation routes form oxides of Fe and Sr in situ and that the reactions from there onwards progress in a similar fashion, ultimately resulting in Sr-hexaferrite. In the case of the coprecipitation method, the ferrite forms with an exothermic reaction at a fairly low temperature, $\simeq 730$ °C, resulting in ultrafine particles.

The reported data on the formation of Ba/Sr hexaferrite has been tabulated in Table 2. All these methods have their own salient processing features such as lypholization, drying at low temperature, high temperature quenching, etc., resulting in various types of intermediate phases; sometimes even amorphous phases have been observed before the ferrite formation. Some of these methods show exothermic change accompanying the ferrite formation, while the others do not.

In the present case, as discussed earlier, both the ceramic and coprecipitation routes follow similar patterns for the ferrite formation. An attempt was

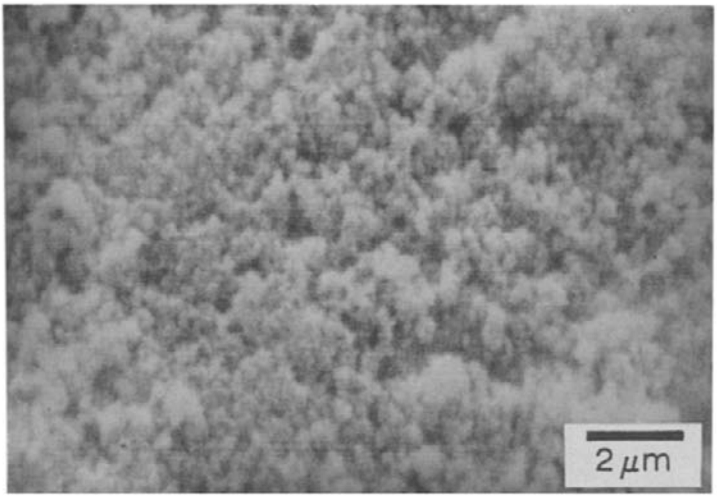

Fig. 8. Scanning electron micrograph of the sample prepared by the coprecipitation route.

TABLE 2

Thermochemical data on the ferritization reaction

Method of preparation	Surrounding atmosphere during reaction	Types of phases detected	Ferritization temp. (°C)	Nature of heat change associated with ferritization	Ref.
Coprecipitation of hydroxides of Ba, Fe	–	Amorphous up to 740 °C, no α-Fe_2O_3 or $BaFe_2O_4$	760	Exothermic	Roos [14]
Coprecipitation by hydrolysis of organometallic precursors of Ba, Fe	Dry N_2	Amorphous at $T \leqslant 750$ °C	750	Exothermic	Higuchi [15]
Liquid mix technique for preparation of citrates of Ba, Fe and their decomposition	$CO + CO_2$	γ-Fe_2O_3, Fe_3O_4, no α-Fe_2O_3	600	–	Srivastava [9]
Gel formation of Ba, Fe and its decomposition	Reducing atmosphere due to burning of organic matter	Amorphous up to 500 °C, Fe_3O_4, γ-$BaFe_2O_4$, no α-Fe_2O_3	700	–	Lucchini [16]
Ceramic method (solid state reaction of $SrCO_3 + \alpha$-Fe_2O_3)	$CO + CO_2$	$SrFe_2O_4$	900	–	Kulkarni [13]
Chemical coprecipitation of hydroxides of Sr, Fe	–	$SrFe_2O_4$	700–730	Exothermic	Date [18] Present work

made to analyse the difference in the thermochemical behaviour of the two methods as follows:

1. The enthalpy of the reaction ΔH ($= q_p$ for reactions at constant pressure), being a state function, depends only on the state of the reactants and products. Because the product, i.e. Sr-hexaferrite, as characterized by XRD and IR, has been found to be exactly identical for both methods, it can be assumed to have same energy state. In contrast, the reactants α-Fe_2O_3 and Sr oxide might have different states because they have been

prepared in situ from two different techniques resulting in different entropy contents. Thus ΔH may vary for the two methods.

2. If during the formation of ferrite, simultaneous processes such as decomposition of the precursor (e.g. $SrCO_3$ decomposing into Sr oxide) with an energy change equal and opposite to that of the ferritization, are in progress, the net effect will be no energy change.

In conclusion, the coprecipitation method forms Sr-hexaferrite at a much lower temperature, with an exothermic energy change. The product thus formed is more uniform with ultrafine particles and exhibits better magnetic properties [13].

ACKNOWLEDGEMENT

We are thankful to Dr. P. Ratnasamy, FNA for many useful discussions and continuing interest in the present work. Thanks are due to Dr. A. Mitra, Mr. M.V. Kuber, Mrs. A.A. Belhekar and Miss M.S. Agashe for their technical assistance.

REFERENCES

1 Tanasoiu, P. Nicolau and C. Miclea, IEEE Trans. Magn., MAG-12 (1976) 980.
2 K. Haneda, C. Miyakawa and H. Kojima, J. Am. Ceram. Soc., 57 (1974) 354.
3 K. Haneda, C. Miyakawa and K. Goto, IEEE Trans. Magn., MAG-23 : 5 (1987) 3134.
4 C.D. Mee and J.C. Jaschke, J. Appl. Phys., 34 (1963) 1271.
5 B.T. Shirk and W.R. Buessem, J. Am. Ceram. Soc., 53 (1970) 192.
6 K. Odo, T. Yoshio, K.O. -Oka and F. Kanamaru, J. Mater. Sci. Lett., 4 (1985) 876.
7 F. Licci and T. Besagni, IEEE Trans. Magn., MAG-20 (1984) 1639.
8 N.G. Eror, Jr., and T.M. Loehr, J. Solid State Chem., 12 (1975) 319.
9 A. Srivastava, P. Singh, V.G. Gunjikar and A.P.B. Sinha, Thermochim. Acta, 86 (1985) 77.
10 B.J.J. Zelinski and D.R. Uhlmann, J. Phy. Chem. Solids, 45 (1984) 1069.
11 Xi-Jing Fan and E. Matijevic, J. Am. Ceram. Soc., 71(1) (1988) C-60.
12 D. Barb, L. Diamandescu, A. Rusi, D. Tarabasanu-Mihaila, M. Morariu and V. Teodorsescu, J. Mater. Sci., 21 (1986) 1118.
13 S. Kulkarni, J. Shrotri, C.E. Deshpande and S.K. Date, J. Mater. Sci., in press.
14 W. Roos, J. Am. Ceram. Soc., 63(11–12) (1980) 601.
15 K. Higuchi, S. Naka and S. Hirano, Adv. Ceram. Mater., 1(1) (1986) 104.
16 E. Lucchini, S. Meriani, F. Delben and S. Paoletti, J. Mater. Sci., 19 (1984) 121.
17 F. Haberey, M. Velicescu and A. Kockel, Int. J. Magn., 5 (1973) 161.
18 S.K. Date, C.E. Deshpande, S.D. Kulkarni and J.J. Shrotri, Fifth International Conference on Ferrites (ICF-5), 1989, in press.
19 C. Duval, Inorganic Thermogravimetric Analysis, 2nd edn., Elsevier, New York, 1963, p. 440.
20 A. Marotta and A. Buri, Thermochim. Acta, 25 (1978) 155.
21 K. Melzer and A. Martin, Phys. Status Solidi A: 107 (1988) K 163, and references therein.
22 A.C. Vajpei, Uma, I.P. Saraswat and K. Chandra, J. Mater. Sci., 19 (1984) 3341.
23 K. Kauffman and F. Hazel, J. Inorg. Nucl. Chem., 37 (1975) 1139.